Mycobacterium tuberculosis secreted antigen (MTSA-10) modulates macrophage function by redox regulation of phosphatases

Article *in* The FEBS Journal · January 2007

DOI: 10.1111/j.1742-4658.2006.05543.x · Source: PubMed

CITATIONS
22

READS
159

7 authors, including:

Sandip K Basu
National Cancer Institute (USA), National Institutes of Health
29 PUBLICATIONS **878** CITATIONS
SEE PROFILE

Dhiraj Kumar
International Centre for Genetic Engineering and Biotechnology
116 PUBLICATIONS **6,907** CITATIONS
SEE PROFILE

Dinesh Kumar Singh
Indian Institute of Toxicology Research
16 PUBLICATIONS **1,310** CITATIONS
SEE PROFILE

Niladri Ganguly
KIIT University
26 PUBLICATIONS **745** CITATIONS
SEE PROFILE

the FEBS Journal

Mycobacterium tuberculosis secreted antigen (MTSA-10) modulates macrophage function by redox regulation of phosphatases

Sandip K. Basu, Dhiraj Kumar, Dinesh K. Singh, Niladri Ganguly, Zaved Siddiqui, Kanury V. S. Rao and Pawan Sharma

Immunology Group, International Centre for Genetic Engineering and Biotechnology, ICGEB Campus, Aruna Asaf Ali Marg, New Delhi, India

Keywords
macrophage dysfunction; MTSA-10; *Mycobacterium tuberculosis*; protein phosphatases; reactive oxygen species

Correspondence
P. Sharma, International Centre for Genetic Engineering and Biotechnology, ICGEB Campus, Aruna Asaf Ali Marg, New Delhi, 110067, India
Fax: +91 11 26162316
Tel: +91 11 26176680
E-mail: pawan37@gmail.com

(Received 7 July 2006, revised 6 October 2006, accepted 17 October 2006)

doi:10.1111/j.1742-4658.2006.05543.x

Macrophages are the primary host cells for *Mycobacterium tuberculosis* (Mtb). Although macrophages can mount a strong inflammatory response to dispose of invading microbial pathogens, the immune dysfunction of the Mtb-infected macrophage constitutes the hallmark of mycobacterial pathogenesis. A 10-kDa, Mtb secretory antigen (MTSA-10), encoded by ORF *Rv3874*, is one of the predominant members of the 'region of difference 1' locus of Mtb genome that has been strongly implicated in mycobacterial virulence. In this study, we investigated the possible role of MTSA-10 in modulating the macrophage dysfunction in a mouse macrophage cell line J774.1. We found that recombinant MTSA-10 caused extensive protein dephosphorylation in J774.1 cells as revealed by two-dimensional gel electrophoresis analysis. We also observed that MTSA-10 treatment downregulated the reactive oxygen species levels in the cells leading to activation of cellular protein phosphatases putatively responsible for the dephosphorylation phenomenon. This implied a direct role of MTSA-10 in the disruption of host cell signaling, resulting in downregulation of transcription of several genes essential for macrophage function.

Mycobacterium tuberculosis (Mtb) is a facultative intracellular microbial pathogen with a strong propensity for invading the macrophages. Subversion of the macrophage immune functions or activation response following its infection with Mtb constitutes the hallmark of mycobacterial pathogenesis [1]. Successful parasitization of macrophages by pathogenic mycobacteria involves modulation of several host cell processes such as surface expression of costimulatory and major histocompatibility molecules [2–5], antigen processing and presentation, maturation of mycobacterial phagosome [6–9], etc., accompanied with underlying nuances in the host cell signaling, which allow Mtb to survive inside the host cells [10]. A 19-kDa lipoprotein of Mtb and a cell-wall component, lipoarabinomannan (LAM), have been implicated in modulation of macrophage functions [11–13]. However, a possible role of Mtb secretory proteins in the modulation of macrophage functions remains to be investigated in detail. We have been studying immunomodulatory role of a 10-kDa, Mtb secretory antigen (MTSA-10 [14]). In Mtb, MTSA-10 and a 6-kDa early secretory antigen target (ESAT-6) are cotranscribed from *Rv3874* and *Rv3875* genes, respectively [15], located in the so-called 'region of difference 1' (RD1) locus of the Mtb genome [16]. The possible role of the RD1 locus in mycobacterial virulence first became apparent from the comparative genomics studies indicating lack of RD1

Abbreviations
DPI, diphenylene iodonium; ESAT-6, 6-kDa early secretory antigen target; IFN, interferon; IPG, immobilized pH gradient; LAM, lipoarabinomannan; LPS, lipopolysaccharide; Mtb, *Mycobacterium tuberculosis*; MBP, myelin basic protein; MTSA-10, *M. tuberculosis* secretory antigen; NAC, *N*-acetylcysteine; pNPP, *para*-nitrophenyl phosphate; PTP, protein tyrosine phosphatase; RD1, region of difference 1; ROS, reactive oxygen species.

in all BCG vaccine strains of *Mycobacterium bovis* [17–19]; several subsequent studies on biogenesis, secretion and immunogenicity of RD1 proteins have directly implicated this locus in mycobacterial pathogenesis and virulence in mice [20–23]. Significantly, targeted deletion of RD1 from Mtb attenuates its virulence in mice [24]; conversely, incorporation of RD1 locus of Mtb into BCG or *Mycobacterium microti*, a natural RD1 deletion mutant, imparts them with enhanced virulence and immunogenicity [21,25]. Mutations in RD1 secretion pathway subverted secretion of ESAT-6 and MTSA-10 and resulted in reduced Mtb replication in cultured macrophages, as the mutants failed to inhibit the macrophage inflammatory responses [22].

We have earlier shown that MTSA-10 can bind to the macrophage surface [26]; subsequently, Renshaw *et al*. [27] have demonstrated that the long flexible arm formed by the C-terminus of MTSA-10 was essential for binding of the MTSA-10:ESAT-6 complex to the cell surface. In the present study, we have examined some aspects of regulation of the host cell signaling by MTSA-10. Here, we demonstrate that MTSA-10 causes extensive dephosphorylation of the macrophage proteins; interestingly, this is accompanied by the downregulation of reactive oxygen species (ROS) generation in the macrophages treated with MTSA-10 leading to enhanced activity of cellular phosphatases and consequent dampening of the macrophage basal signaling machinery.

Results

MTSA-10 causes global dephosphorylation of macrophage phosphoproteome

We have previously shown that MTSA-10 could modulate the macrophage immune functions, possibly by interfering with the signaling machinery of the host cell [14,26]. As phosphorylation and dephosphorylation constitute the key events in cell signaling, we decided to ascertain the role of MTSA-10 in these events. In order to establish the possible involvement of MTSA-10 in the phosphorylation events, J774.1 cells, pre-equilibrated with [^{32}P]-orthophosphoric acid as described in the Experimental procedures section, were exposed to experimentally predetermined optimal dose of purified, lipopolysaccharide (LPS)-free, recombinant MTSA-10 protein. The cell lysates prepared at different time points of incubation were resolved by two-dimensional gel electrophoresis and analyzed by autoradiography.

Results obtained from one such experiment are shown in Fig. 1. Treatment of cells with MTSA-10 resulted in a decrease in the number of detectable phosphoproteins (Fig. 1A, right panel) as compared with those detected in the untreated cells (Fig. 1A, left panel). After normalizing the two autoradiograms for background intensity and analyzing them using the IMAGE MASTER 2D ELITE® software (Amersham Bioscience), we could detect 62 spots, each representing a phosphorylated protein, in the untreated cells, and only 37 in the MTSA-10-treated cells. Seventeen spots appeared to be common in the two panels, while 20 additional spots in the right panel represented *de novo* phosphorylated proteins as a result of MTSA-10 treatment. However, in the presence of MTSA-10, there was an overall decrease in the number of detectable phosphoproteins; this effect was maximal at 20 min after the addition of MTSA-10, and persisted with virtually no change for up to 1 h (data not shown). Interestingly, MTSA-10 treatment resulted in significant dephosphorylation of 58 out of 62 spots seen in the untreated cells. In fact, phosphorylation was undetectable in 45 of the normally phosphorylated proteins.

Data in Fig. 1B,C suggest that MTSA-10 could be exerting substantial signal dampening effect on macrophage signaling machinery as the cells stimulated with MTSA-10 could not maintain the basal phosphorylation status of cellular proteins both in qualitative and quantitative terms. While a large number of proteins failed to maintain their phosphorylated state after MTSA-10 treatment, even the few that could suffered a significant loss in the level of phosphorylation as compared with that observed in the untreated cells.

Supplementary Fig. S1 diagrammatically represents the intensity profile of the individual phosphoprotein spots. It depicts significant reduction in the magnitude of phosphorylation of most proteins following treatment with MTSA-10 (e.g. spots 6, 29, 30, 31, 35 and 53). It also shows that the magnitude of phosphorylation of the new substrates was rather low (e.g. spots 64, 65, 66, 67, 68 and 70), indicating that only a very small pool of these proteins was being phosphorylated. Most importantly, these results indicate that the effect of MTSA-10 was not restricted to any specific subset of target proteins; rather it seemed to be a global phenomenon in which a significant proportion of macrophage proteins were affected.

MTSA-10 treatment regulates macrophage phosphatase activity

The dephosphorylation of macrophage proteins caused by MTSA-10 seemed rather intriguing, especially as we found no evidence of any intrinsic phosphatase activity in MTSA-10. Others have shown that some Mtb

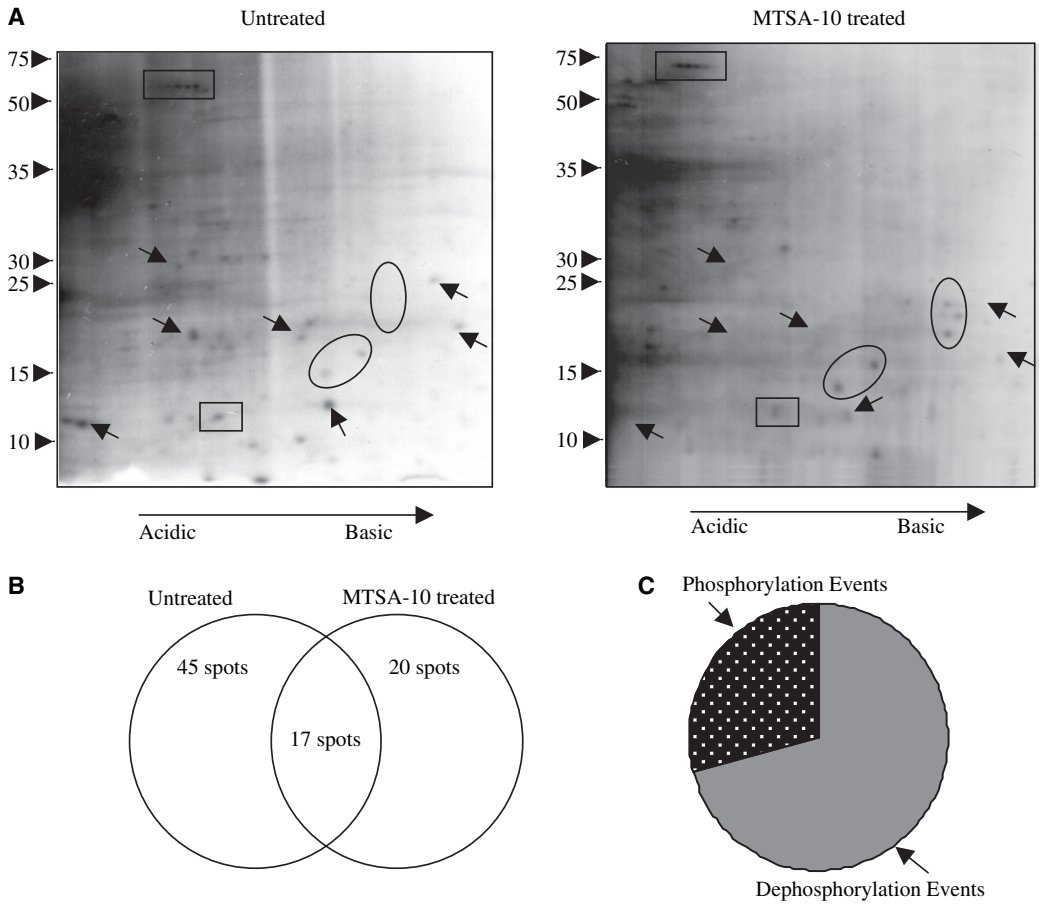

Fig. 1. MTSA-10 dampens macrophage signaling machinery. (A) The autoradiograms obtained upon two-dimensional gel electrophoresis resolution of the phosphorylated proteins from untreated cells and cells treated with MTSA-10 for 20 min. For clarity, only autoradiograms from the region spanning molecular mass range of 10–75 kDa and pI range of 4–7 are shown. The arrowheads indicate some representative spots dephosphorylated by MTSA-10 treatment, while some of those that were phosphorylated by MTSA-10 are enclosed in circles. Spots that remained unchanged by the treatment and are used as internal reference standards for analysis are enclosed in rectangle. (B) Diagrammatic representation of the number of phosphorylation events detected in untreated and MTSA-10 treated cells. (C) Percentage of phosphorylation and dephosphorylation events in MTSA-10-treated cells as compared with untreated cells. All values in (B) and (C) represent the mean of three different experiments.

products like LAM can activate macrophage protein tyrosine phosphatases (PTPs) [12] while, conversely, bacterial lipopolysaccharide is known to inactivate phosphatases. Therefore, we decided to ascertain if MTSA-10 could activate phosphatases and thereby influence the cellular phosphorylation events in the macrophage.

To measure the cellular phosphatase activity upon MTSA-10 treatment, we used a *para*-nitrophenyl phosphate (pNPP) hydrolysis assay for measuring the tyrosine phosphatases, and a phosphopeptide as substrate to measure the serine/threonine phosphatases, as mentioned in the Experimental procedures. It is perhaps pertinent to point out here that pNPP, an artificial protein tyrosine phosphatase (PTP) substrate [28], is not as specific for tyrosine phosphatases as, for example, the 1142–1153 residue insulin receptor peptide [29]; however, as a number of studies have used pNPP for measuring activity of PTPs [30–33], and pNPP has been shown to serve well as a substrate for comparing activities of a newly characterized tyrosine phosphatase HopPtoD2 from *Pseudomonas syringae* and the human lymphocyte antigen-related protein (CD45), a known PTP [34], we have ventured to use pNPP assay as the routine assay for measuring tyrosine phosphatase activity in the present study. We observed that the overall level of phosphatase activity in the cytoplasmic extracts, as measured in a pNPP assay, did not increase significantly during the first 5 min of MTSA-10 treatment, but registered 60% increase by 10 min;

half of this activity could be detected even after 30 min of treatment (Fig. 2A). Interestingly, the serine/threonine phosphatases showed a gradual increase in their enzymatic activity and were found to be 150% more active after 30 min of MTSA-10 treatment as compared with the untreated cells (Fig. 2B).

To study the effect of MTSA-10 on cellular phosphatases in further detail, we selected a subset of nine cellular phosphatases encompassing tyrosine (SHP-1, SHP-2, HePTP and PTP1B), dual specificity (MKP-1 and MKP-2) and serine/threonine phosphatases (PP1, PP2A and PP2B) and monitored their activity upon MTSA-10 treatment. The individual phosphatases were immunoprecipitated from cytoplasmic extracts of MTSA-10-treated cells and were assayed for their activity. The results of one such experiment are shown

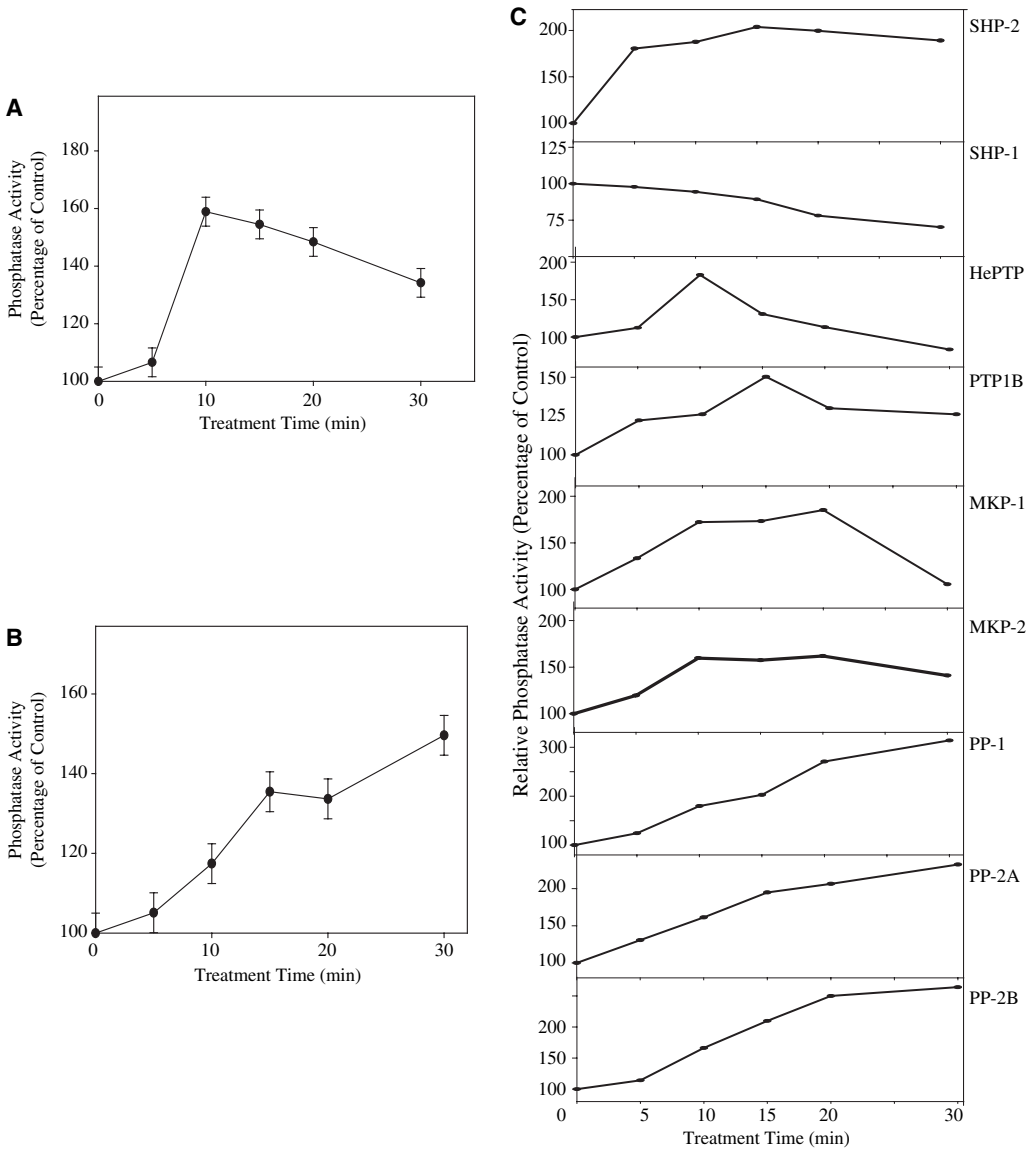

Fig. 2. MTSA-10 activates macrophage phosphatases. Cells (2×10^7/aliquot) were treated with MTSA-10 for indicated time. (A) Cytoplasmic fractions were subjected to an assay for detecting tyrosine phosphatase activity. (B) Cytoplasmic fractions were subjected to an assay for detecting serine/threonine phosphatase activity. (C) Individual phosphatases were pulled down by immunoprecipitation and the immunoprecipitates were subjected to respective phosphatase assay as described in Experimental procedures. In all cases, the activity was shown as percent increase with respect to that obtained in the untreated control cells. In all assays where specific phosphatases were immunoprecipitated, equal protein amounts across various time points were ascertained by western blotting of immunoprecipitates. Data presented in (A) and (B) are the mean ± SD of three separate experiments.

in Fig. 2C. We found that the tyrosine and dual specificity phosphatases reached maximum level of their activity by 10–15 min of treatment; however, by 30 min of MTSA-10 treatment, activity of HePTP decreased to nearly basal level, while others, namely SHP-2, PTP1B, MKP-1 and 2 still remained partially active. A paradox was seen in the case of SHP-1, as its activity moderately decreased upon MTSA-10 treatment. The reason for this decreased activity of SHP-1 is not clear to us as yet.

All the serine/threonine phosphatases, however, showed a gradual increase in their activity with treatment time and were still active at 30 min of MTSA-10 treatment. The kinetics of activation and the level of maximum activity achieved were found to vary between the individual phosphatases (Fig. 2C). The immunoprecipitates obtained with nonspecific antibodies showed negligible phosphatase activity as compared with the untreated cells (data not shown).

The overall message from these experiments was that MTSA-10 upregulated both the tyrosine and serine/threonine phosphatases of macrophage cells, albeit with different kinetics. The overall increase in activity of the cellular phosphatases seemed to be responsible for the global dephosphorylation observed in the cells treated with MTSA-10.

MTSA-10 regulates ROS generation in the macrophage

Phagocytes such as macrophages and neutrophils are specially endowed to produce ROS through activation of NADPH oxidase [35]. Release of ROS, also called 'the respiratory burst', not only helps in killing the pathogen, but also plays an important role in the host cell signaling [36,37]. ROS such as superoxide and hydrogen peroxide (H_2O_2) have been implicated as second messenger molecules in diverse receptor-mediated signal transduction systems, such as epidermal growth factor, platelet derived growth factor, insulin, B cell receptor and T cell receptor [38–40].

Therefore, we next probed the effect of MTSA-10 on ROS generation by J774.1 cells that had been preloaded with an ROS sensitive dye, dichlorodihydrofluorescein diacetate (H_2DCFDA). We found that MTSA-10 could significantly impair the production of ROS by J774.1 cells in a time-dependent manner (Fig. 3A,B), and this inhibition was directly proportional to the concentration of MTSA-10 used (Fig. 3C). As expected, ROS generation by J774.1 cells was markedly inhibited by addition of a NADPH oxidase inhibitor, diphenylene iodonium (DPI), the glutathione peroxidase mimetic, ebselen, and the antioxidant, *N*-acetylcysteine (NAC). It is worthwhile mentioning that MTSA-10 seemed to enhance the effect of all three inhibitors resulting in further downregulation of ROS generation (Fig. 3D). Moreover, as shown in Fig. 3E, we found that the inhibition of ROS generation seemed to be MTSA-10-specific; several other proteins such as chicken egg lysozyme, Mtb secretory antigens Ag85B and ESAT-6, and a *Plasmodium falciparum* merozoite surface protein $MSP1_{19}$ had virtually no effect on ROS generation by J774.1 cells (Fig. 3E).

The fact that MTSA-10 binds to macrophage cell surface [26,27] and our finding that MTSA-10 inhibited the macrophage ROS generation made us wonder if the effect on ROS generation was a result of either MTSA-10 binding to specific cell surface receptor or a physical interaction of MTSA-10 with any key player of ROS metabolism within the cell. To answer this question we checked ROS levels in J774.1 cells that had been stably transfected with *MTSA-10* gene, and constitutively produced MTSA-10 protein within the cells [41]. We found no difference in ROS levels of untransfected (naïve) and MTSA-10-transfected J774.1 cells, as well as trypsin-treated J774.1 cells (Fig. 4A). Interestingly, treatment with MTSA-10 induced a comparable degree of inhibition of ROS in both naïve and MTSA-10-transduced J774.1 cells (Fig. 4B,C). It is also worth mentioning that MTSA-10 had no effect on ROS levels of the trypsin-treated J774.1 cells (Fig. 4D). These data indicated that the macrophage ROS levels were affected by specific binding of MTSA-10 to the cell surface. Significantly, cleavage of the cell surface receptors by trypsin treatment prevented MTSA-10 binding and abrogated its effect on ROS levels. Furthermore, the presence of MTSA-10 constitutively expressed within the cell also had no effect on ROS levels as evident from the comparable ROS levels in naïve and MTSA-10 transfected J774.1 cells. When monitored over time, the effect of MTSA-10 treatment on macrophage ROS levels prevailed at least up to 1 h of treatment (Fig. S2A–F); monitoring for longer period revealed no shift in the ROS levels (Fig. S2A–F).

MTSA-10 has been reported to exist predominantly as MTSA-10–ESAT-6 (1 : 1) complex, with the C-terminal flexible arm of MTSA-10 being essential for binding of the complex to the macrophage cell surface [27]. Therefore, it seemed worthwhile to check the specificity of the effect of MTSA-10 on macrophage ROS generation. We found that ESAT-6, the other counterpart of the complex, had no effect on ROS generation in J774.1 cells (Fig. S3A,B). Interestingly, the J774.1 cells treated with equimolar mixture of ESAT-6 and MTSA-10 exhibited a reduction in the ROS levels which was similar to that obtained with MTSA-10

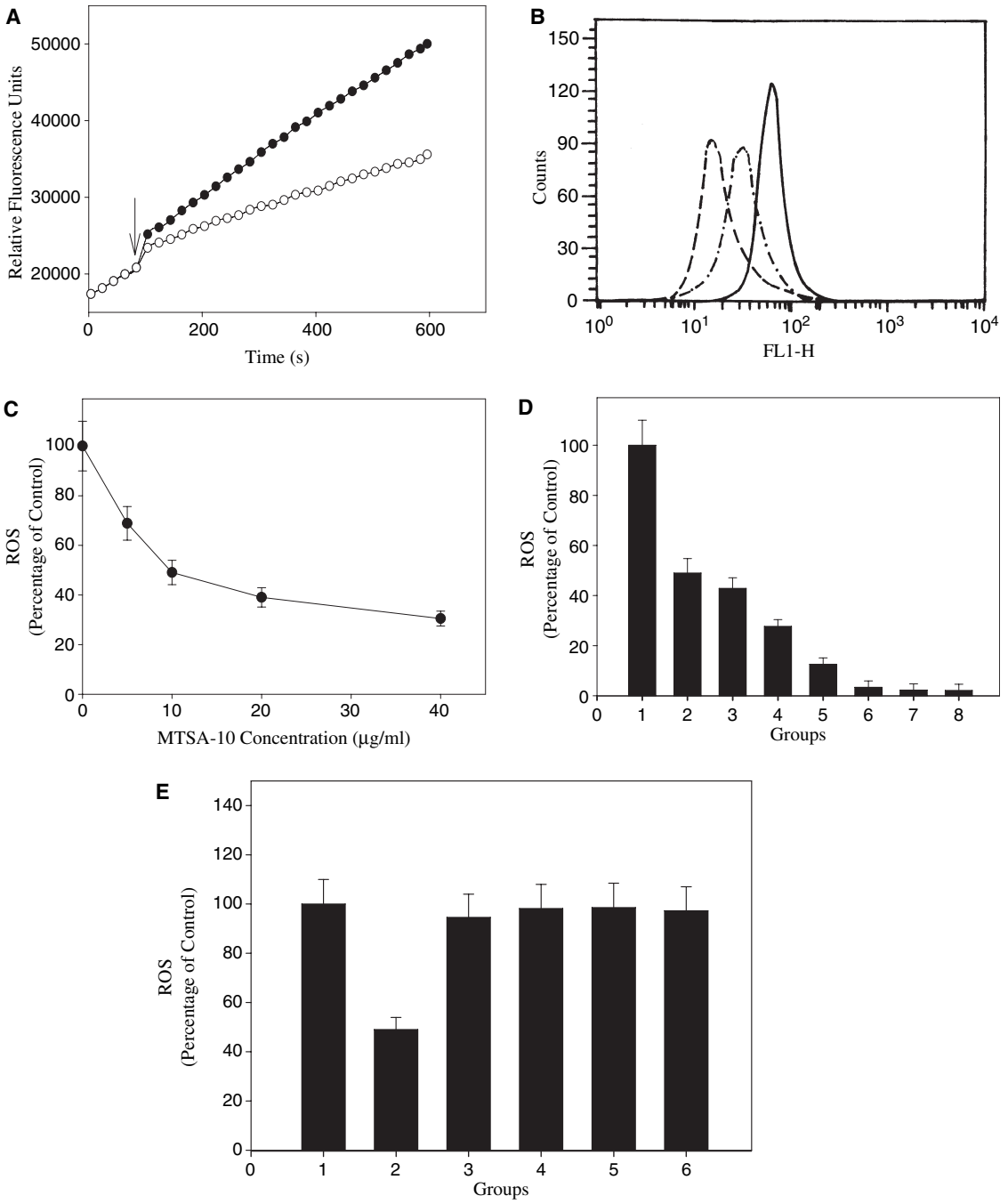

Fig. 3. Effect of MTSA-10 on macrophage ROS generation. (A–E) Profiles of generation of ROS, as measured by H_2DCFDA oxidation are shown. Briefly, H_2DCFDA-labeled J774.1 cells were plated at 1×10^6/100 μL in wells of a 96-well plate, and the fluorescence signal obtained under various conditions was recorded. (A) Results for untreated cells (●) and cells treated with MTSA-10 (○) for indicated time are shown. The arrow indicates the time of addition of MTSA-10. (B) The FACS profile of ROS generation of untreated (——), and cells treated with MTSA-10 for 5 min (–·–) and 10 min (-----) are shown; the cells were preloaded with H_2DCFDA and were subsequently subjected to flowcytometric analysis. (C) The ROS generated by cells treated with different concentrations of MTSA-10 for 10 min are shown. Panel (D) shows relative levels of ROS generation by un-treated cells (without any inhibitor; group 1), and cells treated with MTSA-10 alone (group 2); cells treated with 7.5 μM DPI (group 3), or DPI plus MTSA-10 (group 4); with 50 μM ebselen (group 5) or ebselen plus MTSA-10 (group 6); with 50 mM NAC (group 7) or NAC plus MTSA-10 (group 8). (E) Relative levels of ROS generated by untreated cells (group 1), and cells treated with MTSA-10 (group 2), or 10 $\mu g \cdot mL^{-1}$ each of lysozyme (group 3), $MSP1_{19}$ (group 4), ESAT-6 (group 5) and Ag85-B (group 6) are shown. In (E), the values are the mean ± SD of three different experiments.

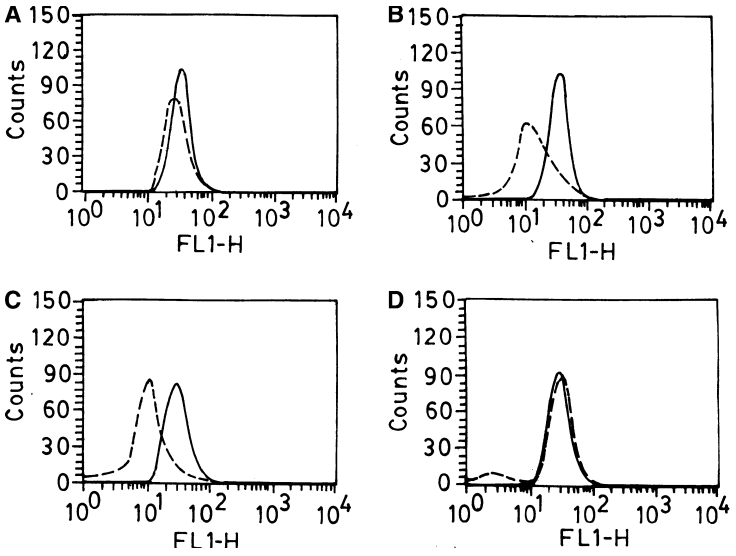

Fig. 4. Reduction of macrophage ROS generation needs binding of MTSA-10 on cell surface. (A–D) The FACS profiles of ROS generation as measured by H_2DCFDA oxidation are shown. The profiles shown in (A) represent ROS levels seen in untreated, untransfected J774.1 cells (——), MTSA-10-transfected cells (·····), and the trypsin-treated, untransfected cells (----) [(·····) is masked by (-----)]. (B) shows the FACS profiles of ROS in untransfected, untreated J774.1 cells (——) and in the cells treated with MTSA-10 for 10 min (-----). (C) shows profiles of ROS in MTSA-10-transfected but untreated cells (——) and MTSA-10 treated cells (-----). (D) shows profiles of ROS in untransfected trypsin-treated J774.1 cells (——) and trypsin plus MTSA-10 treated cells (-----). Data presented is from one of three different experiments with reproducible results.

alone (Fig. S3C), or with the MTSA-10–ESAT-6 (1 : 1) complex (Fig. S3D) prepared according to Renshaw *et al.* [38]. These results suggest that MTSA-10 alone had similar effect on the macrophage ROS generation as the MTSA-10–ESAT-6 (1 : 1) complex, and therefore MTSA-10 in the complex was per se responsible for this effect.

Furthermore, we obtained similar inhibitory effect of MTSA-10 on ROS generation in another murine macrophage cell line, RAW 264.7, as well (Fig. S4A). Since nitric oxide scavenger, L-*N*-monomethyl arginine had no effect on MTSA-10-dependent ROS inhibition (Fig. S4B), MTSA-10 seemed to directly affect macrophage ROS generation or its half-life, and not the feeder pathway via nitric oxide.

Also, we validated the inhibitory effect of MTSA-10 in the primary macrophage cultures. As shown in Fig. S5, treatment of mouse peritoneal macrophages with MTSA-10 led to reduction in ROS levels, while ESAT-6 treatment had no detectable effect. In line with our previous observation, in the peritoneal macrophages treated with a physical mixture of MTSA-10 and ESAT-6, as well as in those treated with MTSA-10–ESAT-6 (1 : 1) complex, we observed a reduction in the ROS levels as compared with the untreated cells. This indicates that the effect of MTSA-10 over ROS level is a general phenomenon observed in macrophages.

MTSA-10 regulates macrophage phosphatase activity in a ROS-dependent manner

Redox-regulatory mechanisms have been implicated in activation of several receptor tyrosine kinases, basically via inactivation of receptor associated phosphatases [42]. Conversely downregulation of ROS generation could allow PTPs to stay enzymatically active and thereby prevent phosphorylation by protein tyrosine kinases. The ROS oxidize the redox-regulated cysteine in the catalytic site of the tyrosine phosphatase, rendering the latter inactive [38,43], while inactivation of the Ser/Thr phosphatase results from oxidation of a redox sensitive binuclear metal ion centre in their catalytic site, as documented in the case of calcineurin [44,45]. To establish whether any correlation existed between the decreased level of ROS and an elevated degree of phosphatase activity in MTSA-10 treated cells, we immunoprecipitated each of the nine phosphatases selected earlier (viz., HePTP, SHP-2, SHP-1, PTP-1B, MKP-1, MKP-2, PP-1, PP-2A, and PP-2B) and studied their activity under different treatment conditions.

In Fig. 5A, we present the results of an experiment in which immunoprecipitates from untreated control cells (group 1) and those treated as indicated (groups 2–7) were assayed for phosphatase activity. Treatment of immunoprecipitates with a reducing agent, dithiothreitol (group 2) resulted in a marked increase in the enzyme activity of all nine phosphatases as compared with the untreated controls. This result indicated that in the macrophage, the basal level of phosphatases was maintained by their oxidation, so that their treatment with dithiothreitol, leading to reduction of the catalytic site cysteine, led to an increase in their phosphatase activity. A similar albeit less pronounced result was obtained with NAC (50 mM) treatment (group 3), although the magnitude of increase in the enzyme activity varied for different phosphatases. Immunoprecipitates of cells treated with MTSA-10 for 10 min (group 4) displayed a similar trend of increase in

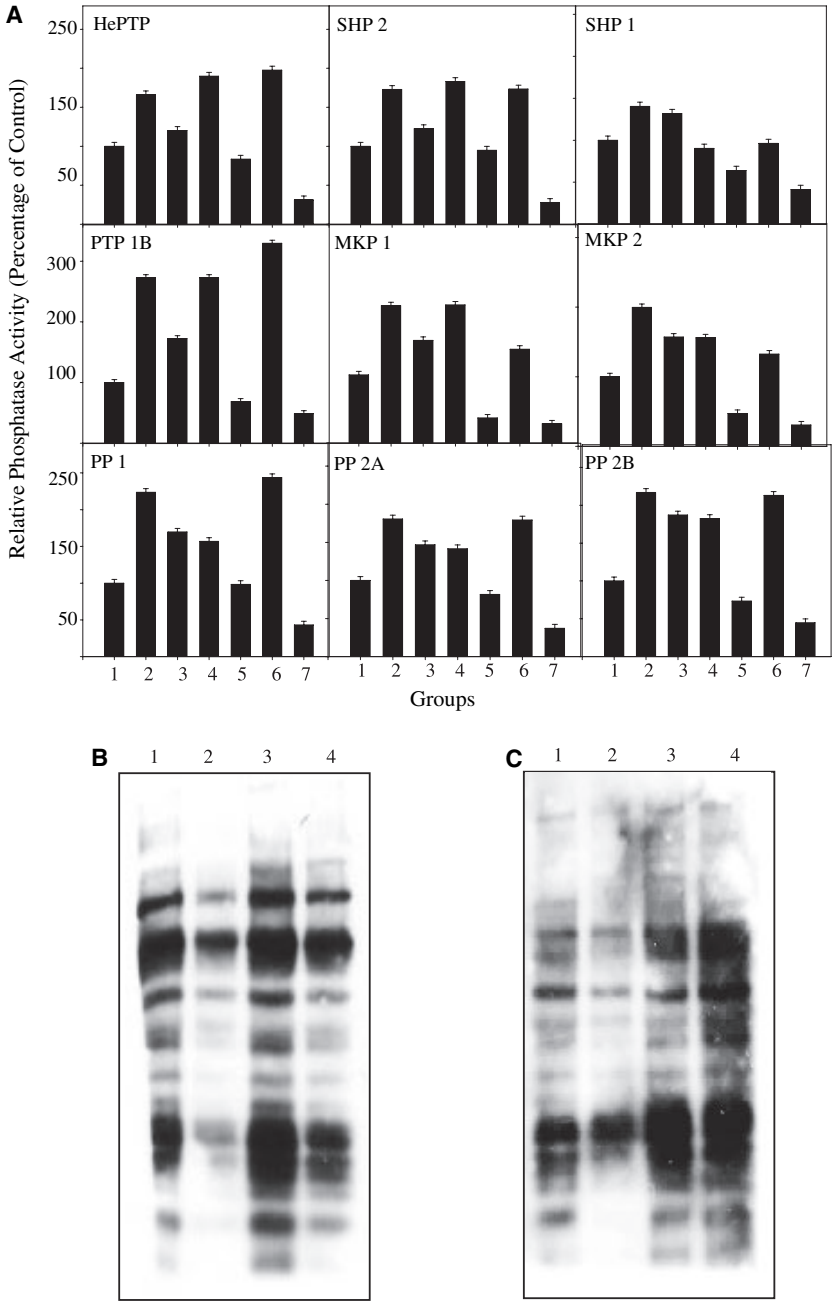

Fig. 5. Reduction of ROS by MTSA-10 is the cause for the activation of macrophage phosphatase. (A) shows relative activity of individual phosphatases immunoprecipitated from untreated cells (group 1), immunoprecipitate treated with 1 mM dithiothreitol prior to the phosphatase assay (group 2) and from cells pretreated with 50 mM NAC (group 3). The immunoprecipitation was carried out from cells treated with MTSA-10 for 10 min (groups 4, 5 and 6) where the cells were supplemented with H_2O_2 (group 5) or pretreated with 50 mM NAC (group 6). Group 7 shows the phosphatase activity of the immunoprecipitates obtained with non-specific antibodies. In all cases, the activity shown represents the percent increase with respect to the untreated control cells. (B) and (C) show western blots of the total cellular proteins from untreated cells (lane 1) and cells treated with MTSA-10 for 20 min (lanes 2, 3 and 4); additionally, cells were supplemented with H_2O_2 (lane 3), or treated with sodium orthovanadate (lane 4 in B) or okadaic acid (lane 4 in C). Proteins were fractionated by SDS/PAGE and probed with anti-phosphotyrosine (B) or anti-phosphoserine/threonine sera (C).

activity of all but one (SHP-1) phosphatases, which was reversed by supplementation with H_2O_2 (group 5) or enhanced by priming with NAC (group 6). Consistent with the activity profile shown in Fig. 2C, the tyrosine phosphatase SHP-1 displayed decreased activity upon MTSA-10 treatment. These results demonstrate that the activity of phosphatases from the cells could be independently enhanced either by treatment with a reducing agent or by bringing down the level of oxidant species in the cell. This experiment also tends to suggest that MTSA-10 (group 4) helped increase the cellular phosphatase activity by reducing the level of ROS in the cell as its effect could be reversed by supplementation with an oxidant species in the form of H_2O_2 (group 5). A careful analysis of the results presented in Fig. 5A, however, reveals subtle variation in the level of activation of oxidized PTPs as an effect of MTSA-10; thus, MTSA-10 did not seem to significantly affect phosphatase activity of MKP-1 and 2 in the NAC-pretreated cells (group 3 versus 6), while in the case of HePTP, SHP-2 or PTP-1B, we found that MTSA-10 further enhanced their phosphatase activity

in the NAC-pretreated cells (groups 3 versus 6), indicating alternative ways of regulation of these (MKP1 and MKP2) phosphatases.

Results presented in Fig. 5B,C provide evidence for a possible correlation between increase in phosphatase activity due to reduction in ROS levels and global dephosphorylation caused by MTSA-10 treatment. Treatment of cells with MTSA-10 reduced the overall protein tyrosine phosphorylation level (Fig. 5B, lane 2), as compared with untreated cells (Fig. 5B, lane 1); this effect could be reversed independently either by supplementation of ROS in form of H_2O_2 (Fig. 5B, lane 3), or by preinactivation of cellular tyrosine phosphatases by sodium orthovanadate prior to MTSA-10 treatment (Fig. 5B, lane 4). Similarly, the reduced levels of the serine/threonine phosphorylation in MTSA-10-treated cells (Fig. 5C, lane 2), as compared with untreated cells (Fig. 5C, lane 1), can also be reverted back either by H_2O_2 treatment (Fig. 5C, lane 3) or by inactivation of serine/threonine phosphatases by okadaic acid prior to MTSA-10 treatment (Fig. 5C, lane 4).

Together these results show that the dephosphorylation observed with MTSA-10 treatment was indeed due to the reduction in ROS levels caused by MTSA-10 treatment leading to higher levels of cellular phosphatases and consequent dephosphorylation of the cellular proteins.

MTSA-10 regulates macrophage downstream signaling and gene expression in a ROS-dependent manner

A key strategy used by pathogens to survive in a hostile environment is to interfere with normal cell signaling in order to disable the host cell defenses. Different bacterial pathogens use diverse strategies to achieve a common goal of undermining host-cell functions and thereby establishing a permissive niche for themselves [46,47]. Mtb, being one of the most successful pathogens, employs more than one strategy for its own benefit by differential regulation of host cell signaling [10]. Mitogen-activated protein kinase (MAPK) signaling pathway is one of the most important cellular targets of Mtb. While pro-inflammatory cytokine interferon (IFN)-γ induces activation of ERK1/2 at the distal end of MAP kinase pathway leading to induction of *NOS-2* gene expression [48], LAM of Mtb is known to limit ERK1/2 phosphorylation in THP-1 cells [12]. Nonpathogenic mycobacteria generally induce sustained activation of MAP kinase in infected macrophages while virulent *Mycobacterium avium* induces a rapid loss of the MAP kinase activity [49].

In view of our observations indicating dephosphorylating activity of MTSA-10, it seemed plausible to explore whether MTSA-10 was affecting specific macrophage signaling pathways. So, we next investigated the intracellular signaling events putatively affected by MTSA-10, taking ERK1/2 as a model indicator molecule for the downstream signaling along the MAPK pathway, a favorite target of pathogenic mycobacteria [12,49]. We found that MTSA-10 induced rapid dephosphorylation of ERK1/2 in the cytoplasm, as phospho-ERK1/2 became virtually undetectable by 30 min of MTSA-10 treatment. This effect was limited to dephosphorylation only, as equivalent amount of ERK1/2 was detected through the entire time course of the experiment (Fig. 6A). Interestingly, exogenous supply of ROS in the form of H_2O_2 could effectively prevent MTSA-10 from dephosphorylating ERK1/2 (Fig. 6A), indicating that dephosphorylation could, indeed, be a result of MTSA-10-dependent ROS inhibition. Furthermore, addition of a PTP inhibitor, sodium orthovanadate, restored the phosphorylation state of ERK1/2 (Fig. 6A), corroborating that dephosphorylation of ERK1/2 was being mediated through MTSA-10 induced protein phosphatases activation. In mouse peritoneal macrophages as well, MTSA-10 induced dephosphorylation of ERK in the cytoplasm without affecting the ERK protein levels (Fig. S5E).

Next, we studied the effect of MTSA-10 on the kinase activity of ERK1/2 (Fig. 6B–D). For this study, ERK1/2 was immunoprecipitated from MTSA-10-treated cells and its kinase activity was measured using myelin basic protein (MBP) as the substrate. Treatment with MTSA-10 resulted in gradual inactivation of ERK1/2 kinase activity, with maximum inactivation observed at 45 min after addition of MTSA-10. Importantly, this inactivation could be reversed with exogenous ROS supplied in the form of H_2O_2, which was found to be comparable with the ERK activity observed in cells treated with H_2O_2. This again indicated that reduction in ROS level brought about by MTSA-10 was playing a key role in ERK1/2 inactivation (Fig. 6B). Treatment of the cells with an increasing concentration of MTSA-10 led to a corresponding decrease in ERK kinase activity indicating that MTSA-10 induced the inactivation of ERK1/2 in a dose-dependent manner (Fig. 6C). In addition to the magnitude of enzyme activity, ERK1/2 obtained from MTSA-10-treated cells also displayed a reduction in kinetics of substrate phosphorylation (Fig. 6D). MTSA-10 treatment resulted in a 2.5–3-fold reduction in the rate of substrate phosphorylation. Thus, MTSA-10 seemed to directly regulate the proportion of

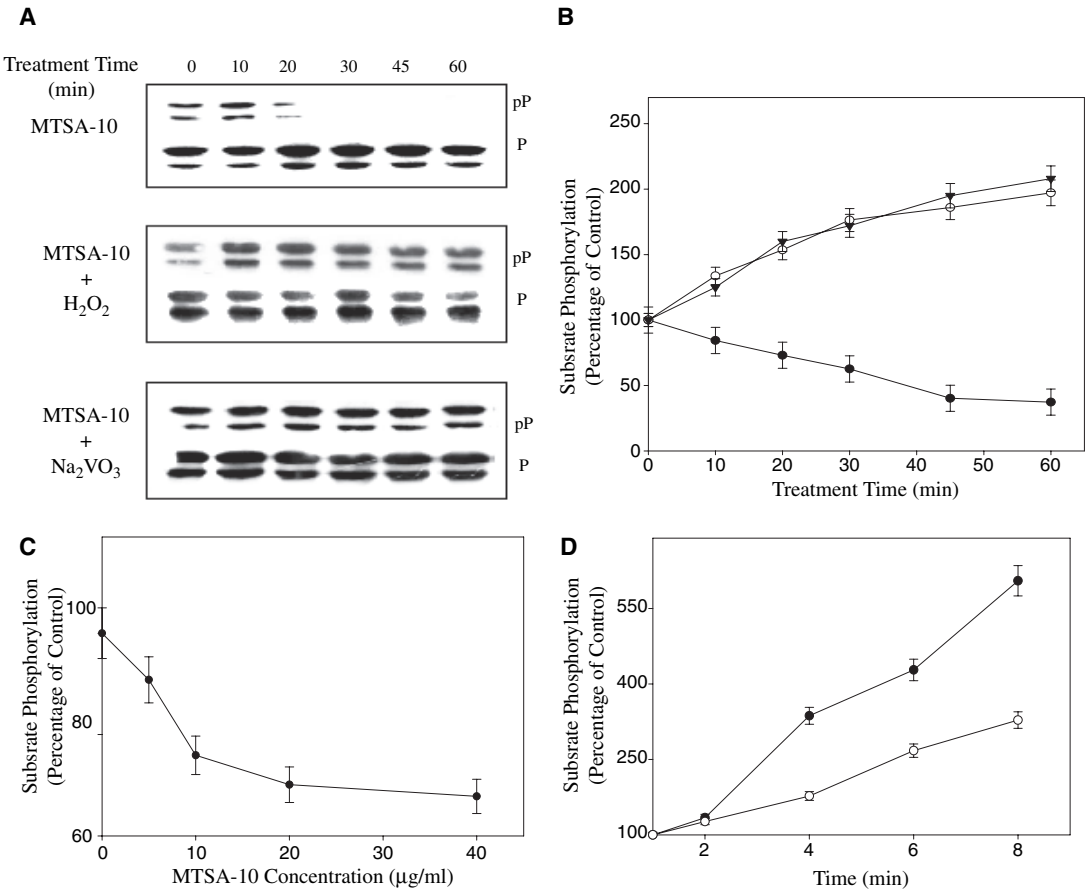

Fig. 6. Effect of MTSA-10 on ERK activity. (A) Cells were treated for the indicated time with MTSA-10 alone or in the presence of H_2O_2 or sodium orthovanadate (1 mM each). Phosphorylation status of ERK1/2 was examined by western blotting followed by probing with anti-phospho-ERK sera. (B) ERK1/2 was immunoprecipitated from cells (1×10^7/group) treated with MTSA-10 in the absence (●) or presence of H_2O_2 (○) and also from cells treated with H_2O_2 alone (▼). These immunoprecipitates were then employed in a kinase assay using MBP as substrate. Results show the net incorporation of radioactive phosphate in the substrate after background subtraction. (C) Cells were treated with different concentrations of MTSA-10 for 30 min and ERK was immunoprecipitated from each group and subjected to kinase assay. (D) ERK was immunoprecipitated from untreated cells (●) and cells stimulated by MTSA-10 (○) for 30 min. The immunoprecipitates obtained were used in substrate phosphorylation assay where substrate phosphorylation was monitored as a function of time. Values shown represent the time-dependent increase in MBP phosphorylation. All values were expressed as percent increase in respect to the untreated cells as control. Whereas (A) is representative of four different experiments, values in (B), (C) and (D) are mean ± SD of three experiments.

ERK1/2 molecules available for activation. This, in turn, regulated both the extent and the rate of substrate phosphorylation mediated by this kinase.

Cellular signaling has direct implications for transcriptional changes in the nucleus in eukaryotic cells. The cell-specific gene expression involves a cascade of controls over transcription factors and the signals that activate these factors [50]. Mtb is known to reprogram macrophage transcriptome for its own benefit and to suppress transcription of a large number of macrophage genes considered essential for the host cell activation [51,52]. A direct repercussion of its impact on cellular signaling was reflected in the way MTSA-10 was found to modulate the macrophage gene expression. A selected subset of genes considered essential for macrophage activation and its primary role as an antigen-presenting cell, was analyzed by RT-PCR amplification for their expression in the cells treated with MTSA-10 (Fig. 7A,B). We found that MTSA-10 downregulated transcription of genes essential for response to activation molecules such as tumor necrosis factor-α and IFN-γ, as well as those encoding costimulatory molecules CD80 and CD86 (Fig. 7A). This effect was time-dependent, as longer incubation with MTSA-10 augmented the magnitude of downregulation.

In view of our other results, we then asked the question whether this effect on gene expression was indeed

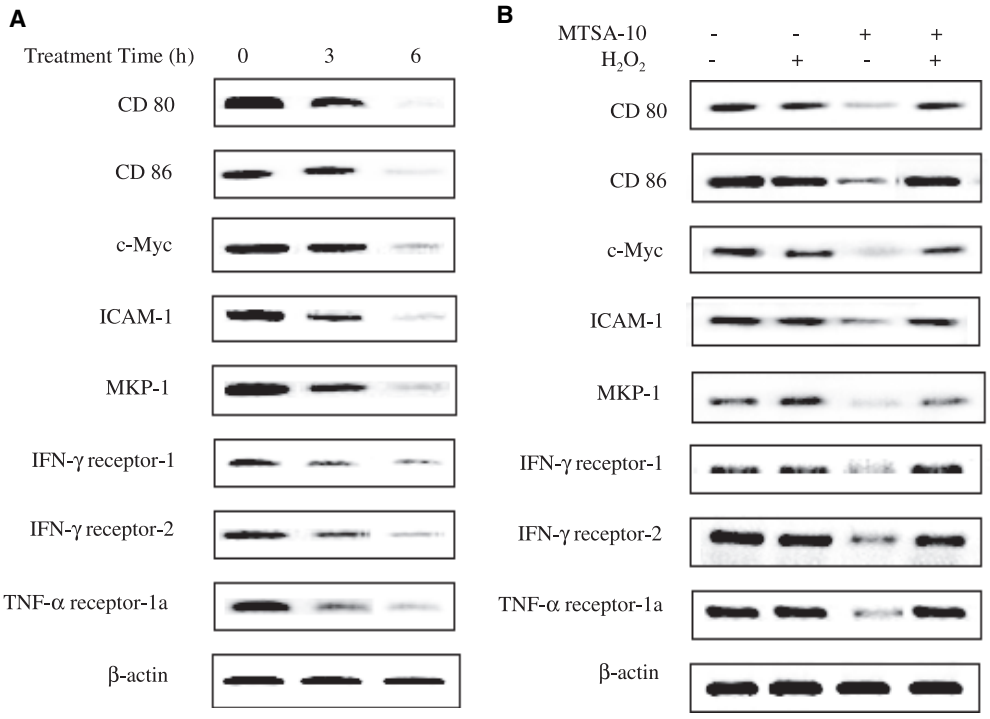

Fig. 7. MTSA-10 regulates macrophage gene expression by a ROS-dependent mechanism. Profiles of mRNA level of different genes as obtained by RT-PCR are shown. Cells (1×10^6/group) were treated with MTSA-10 for indicated time in (A) and for 6 h in the presence or absence of H_2O_2 in (B). Total RNA was isolated from each group and was subjected to RT-PCR with primers specific for the genes indicated. Data shown are representative of three different experiments.

a result of basal signal dampening due to inhibition of ROS caused by MTSA-10 leading to PTP inactivation. We therefore treated cells with MTSA-10 after exogenous ROS supplementation in the form of H_2O_2. The presence of ROS led to reversal of downregulation of gene transcription (Fig. 7B). This result indicated that inhibition of ROS generation, caused by MTSA-10, not only affected macrophage signaling, but also disabled the macrophage to maintain its basal gene expression level.

Discussion

The most important observation of the present study relates to the striking dephosphorylation of macrophage proteins by a mycobacterial secretory protein, MTSA-10, leading to disruption of host cell signaling. While bacterial pathogens are known to disrupt host-cell signaling [1], global dampening of macrophage signaling machinery seen in the presence of MTSA-10 was unexpected. At least within the time frame of our experiment, MTSA-10-treated macrophages failed to maintain or recover their basal phosphorylation status. The dephosphorylation events, which had peaked by 20 min of treatment, were found to be more dominant both quantitatively and qualitatively than the phosphorylation events. This dephosphorylation of cellular proteins is apparently due to the increased activity of cellular phosphatases observed as a result of MTSA-10 treatment. It was found that the kinetics of activation of tyrosine and serine/threonine phosphatases varies, and though some reach the basal activation level by 30 min of treatment, others still remain active. Together they did not allow the treated macrophages to recover their basal phosphorylation status, even after 60 min of MTSA-10 treatment.

Another important result we obtained was that MTSA-10 brought down levels of oxidant species in macrophages. Importantly, ROS levels dropped rapidly within seconds of addition of MTSA-10, and this decline persisted for at least up to 1 h of treatment, making this effect fairly stable. Furthermore, the inhibitory effect of MTSA-10 on macrophage ROS was dose dependent, indicating a system that could display a graded shift in its steady state equilibrium. Our results also showed that the binding of MTSA-10 on the macrophage surface was necessary to bring about the changes in ROS levels; the physical presence of MTSA-10 within the cell had no effect on ROS levels as observed in the transfected cells. Our unpublished

preliminary observations also suggest that MTSA-10 treatment did not have any appreciable effect on macrophage superoxide generation as measured by dihydroethidium oxidation. These results together suggested that binding of MTSA-10 on the cell surface might be accelerating the process of breakdown of hydrogen peroxide to oxygen and water and thereby reducing the level of available H_2O_2 in the cell. However, it needs more work to understand the exact mechanism of reduction in ROS levels by MTSA-10.

The reduction in ROS levels due to MTSA-10 treatment of cells was the likely cause for increased activity of the phosphatases and consequent decrease in both tyrosine and serine/threonine phosphorylation of the cellular proteins. As the effect of MTSA-10 on ROS levels stayed for over an hour, it seemed to facilitate some of the phosphatases to remain active even after 30 min of MTSA-10 treatment, and to maintain the dephosphorylated status of the macrophage cellular proteins over the period of one hour, the time frame of our experiments. However, a marked exception was observed in the case of tyrosine phosphatase SHP-1, which suffered a moderate decrease in its activity following MTSA-10 treatment of the cells. Although the role of two SHPs both as positive and negative regulators of cellular signaling has been shown [53–55], the cause of preferential inactivation of SHP-1 in our studies is presently not clear to us. However, we assume that there might be a secondary level of regulation in case of SHP-1, where another not-yet-identified phosphatase, activated by MTSA-10, might be inactivating SHP-1. Further detailed study is necessary to understand the regulatory mechanism of this phosphatase. In any event, ROS-mediated phosphatase inactivation has been noted during activation of several receptor systems, which strongly suggest that inactivation of phosphatases is sufficient to shift the balance in favor of signal activation [35,36]. Alternatively, as our present results suggest, activation of phosphatases can shift the balance in favor of signal inactivation.

The dephosphorylation effect of MTSA-10 percolated to downstream signaling molecules, as evident in the case of ERK phosphorylation at the furthest point of MAP kinase pathway. It was also evident that this effect of MTSA-10 could be neutralized by elevation of ROS levels or inhibition of phosphatases. The ROS suppression, caused by MTSA-10, attenuated both the magnitude and kinetics of substrate phosphorylation by ERK. Because ERK, along with other effector molecules, carries the signal to the nucleus, we are inclined to think that it is the effect of ROS on signal activation that impacts subsequent gene expression. As our data suggested, it was the effect of MTSA-10 on ROS generation that compromised macrophage in its physiological function; while sustained stimulation with MTSA-10 could lead to further downregulation of the activation markers and early response genes, external supply of ROS fully overcame this effect. This indicates that the inhibition of ROS generation by MTSA-10 was the 'control switch' that tuned the consequent downstream effects.

Not being equipped to produce OxyR, a critical constituent of the oxidative stress response as in other intracellular bacteria like *Escherichia coli* and *Salmonella typhimurium,* Mtb seems to have armed itself with a host of components to deal with ROS or oxidative stress, such as a catalase peroxidase, KatG [56,57], and two superoxide dismutase proteins, SodA and SodC [58,59]. Our present study indicates that a secretory protein like MTSA-10 can also downregulate ROS generation in the cultured macrophages. More work will be required to establish relevance of these observations in the Mtb–macrophage interaction, using Mtb mutants.

MTSA-10 has been reported to exist predominantly as part of the 1 : 1 complex of MTSA-10 and ESAT-6 [27,60]. Conversely, Gao *et al*. [61] have provided evidence for discordance between secretion of ESAT-6 and MTSA-10; their findings indicated that complexation between these two molecules was not required for secretion of MTSA-10. It is evident from the present study that the binding of MTSA-10 alone to the cell surface exerted an inhibitory effect on the macrophage ROS generation that was similar to the one obtained with the MTSA-10–ESAT-6 complex (Fig. S3A,D). Our findings suggest that it is MTSA-10 in the complex that plays the role of modulator of immune function. The study of regulation of macrophage signaling by MTSA-10 can thus extend our knowledge, at least to some extent, as to how the MTSA-10–ESAT-6 complex might regulate the macrophage functions. Interestingly, a recent study has found that human T-cell responses to the MTSA-10–ESAT-6 complex were inferior to those induced with ESAT-6, and that these were only as good as those achieved with MTSA-10 alone [62]. Furthermore, MTSA-10 was responsible for preventing digestion of the MTSA-10–ESAT-6 complex with lysosomal enzymes (cathepsins L and S), suggesting inhibitory/regulatory role of MTSA-10 in the antigen processing [62]. It may be pertinent to point out that Okkels *et al*. [63] have reported presence of as many as eight species of ESAT-6 in Mtb short-term culture filtrate; three of these were acetylated and showed preferential binding of MTSA-10. This observation also raises the possibility that at least some proportion of MTSA-10 and ESAT-6 may, indeed, exist as independent moieties, potentially

capable of exerting their individual influence on the host cell responses.

In conclusion, this study presents evidence for the ability of a Mtb secretory protein, MTSA-10, to modulate cell signaling by activating phosphatases through downregulation of innate ROS levels in the cultured host cell. However, a number of questions remain to be addressed; for example, a detailed characterization of this novel interaction between MTSA-10 and the host cell must be carried out with deletion mutants of Mtb in primary macrophage cultures. Furthermore, a study on possible impact of immune effector molecules like IFN-γ and tumor necrosis factor-α on the MTSA-10–macrophage interaction will be required to gain a better perspective on this interaction.

Experimental procedures

Cell lines and reagents

A mouse tumor-derived macrophage-monocyte cell line J774A.1 and a murine macrophage-like cell line RAW264.7, originally obtained from the American Type Culture Collection (ATCC; Manassas, VA, USA), were procured from the National Centre for Cell Science (Pune, Maharashtra, India), and maintained in DMEM (Life Technologies, Carlsbad, CA, USA) supplemented with 10% heat-inactivated fetal bovine serum (Life Technologies), at 37 °C in 5% CO_2.

Affinity-purified, LPS-free, recombinant 6xHis-tagged MTSA-10 protein, cloned in bacterial expression vector pQE-31 (Qiagen, Valencia, CA, USA), was prepared as described [26]. Recombinant ESAT-6 and Ag85B proteins of Mtb were also expressed and purified in-house following standard procedures ([65]; A. Grover and P. Sharma, unpublished data). Purified recombinant 19-kDa fragment of *P. falciparum* merozoite surface protein-1 ($PfMSP\text{-}1_{19}$), cloned in pQE vector system, was a kind gift from P. Malhotra (Malaria Research Group, ICGEB, New Delhi, India). QIAexpressionist® protein expression and purification kit including Ni-NTA-Agarose, gel purification kit and all primers used for amplification of c-DNA were from Qiagen. Protein A-agarose, 5-bromo-4-chloro-3-indolyl-beta-D-galactopyranoside (X-gal), isopropyl-thio-D-galactopyranoside, ampicillin, kanamycin, pNPP, DPI, NAC, Ebselen, L-N^G-monomethyl arginine (L-NMMA), dephosphorylated casein, MBP, sodium orthovanadate (Na_3VO_4), sodium fluoride, aprotinin, pepstatin, leupeptin, iodoacetamide were purchased from Sigma (St Louis, MO, USA). Bacto tryptone, yeast extract and Bacto agar were from Difco (San Diego, CA, USA). Immobilized pH gradient (IPG) dry-strips, dithiothreitol and other chemicals used for two-dimensional gel electrophoresis were from Amersham Biosciences (Uppsala, Sweden). H_2DCFDA and dihydroethidium were from Molecular Probes (Eugene, OR, USA). IL-12p40 detection ELISA kit was from BD Pharmingen (San Diego, CA, USA). The serine/threonine phosphatase assay kit was from Upstate (Charlottesville, VA, USA). All the antibodies used for immunoprecipitation, western blotting, and the enhanced chemiluminescence kit were from Santa Cruz Biotechnology (Santa Cruz, CA, USA). [^{32}P]-Orthophosphoric acid was from Perkin-Elmer (Boston, MA, USA).

Treatment of cells with MTSA-10 and the resolution of phosphorylated proteins by two-dimensional gel electrophoresis

J774A.1 cells (1×10^7) were placed in phosphate-free DMEM supplemented with 1% fetal bovine serum for 2 h before [^{32}P]-orthophosphoric acid (0.5 mCi·mL^{-1}) was added and the incubation continued for an additional 4–5 h. One set of these cultures was then treated with affinity purified, LPS-free, recombinant MTSA-10 protein at a final concentration of 10 μg·mL^{-1} for indicated time while another set received no such treatment and served as control. The cytoplasmic fractions of cell lysates were prepared and resolved by two-dimensional gel electrophoresis, which was performed essentially as described elsewhere [64], using IPG strips (Amersham Biosciences). Briefly, J774.1 cells from the MTSA-10- or mock-treated cultures were harvested and washed once with culture medium by centrifugation, disrupted in the lysis buffer (8 M urea, 4% Chaps and 2% (v/v) IPG buffer pI 4–7), and their cytoplasmic fractions obtained by ultracentrifugation. The cell extracts corresponding to different time points were diluted in rehydration buffer (8 M urea, 2% (v/v) Chaps, 0.28% (w/v) dithiothreitol, 0.5% (v/v) IPG buffer pI 4–7), and applied to IPG strips, pI 4–7, using the 'in-gel rehydration' method. The isoelectrofocusing was performed in the IPGphor isoelectrofocusing system (Amersham Biosciences), with the following voltage program: gradient from 0 to 500 V in 2 h, 500 V constant for 5 h, gradient from 500 to 4000 V in 2 h, step up to 4500 V and hold for 1 h, and finally step up to 5000 V constant until 22–24 kVh. Later, IPG strips were equilibrated in solutions A (50 mM Tris/HCl, pH 8.8 containing 6 M urea, 30% glycerol, 2% SDS, 1% dithiothreitol) and B (solution A without dithiothreitol, but with 2.5% iodoacetamaide and 0.005% bromophenol blue). Each strip was then loaded on to top of a SDS/PAGE slab (12% gel, 1-mm thick) and electrophoresis was performed at a constant current of 20mA per gel, to resolve the focused proteins in the second dimension.

The resultant gels were silver stained to ascertain that comparable quantities of proteins from experimental and control groups were loaded for analysis. Dried gels were then exposed to X-ray films. Phosphoproteins were visualized by autoradiography and digitized on a Molecular Dynamics computing densitometer using IMAGE QUANT software, version 5.2, and were analyzed using IMAGE MASTER 2D software version 4.01 (Amersham Biosciences).

Only spots with an area greater than 75 pixels were considered, and the minimum intensity surrounding the spot on the film was taken as its background and subtracted to give the true intensity. Relative quantification was achieved by normalizing against three distinct spots that were unaffected upon stimulation of cells. Calibration for the molecular mass and pI was carried out on the basis of standard markers that were run on parallel gels.

Cellular fractionation and phosphatase assay

Following incubation of J774.1 cells with MTSA-10 for indicated time, for assessment of tyrosine phosphatases, cells were lysed for 20 min at 4 °C in lysis buffer (10 mM Hepes, pH 7.4, 10% glycerol and 10 $\mu g \cdot mL^{-1}$ each of aprotinin and pepstatin). The phosphatase assay was done using pNPP as substrate as described earlier [66]. Briefly, 20 μg of total protein fraction or the immunoprecipitates were incubated in assay buffer (5 mM Mes, pH 6.4, 1 mM EDTA pH 8.0, 0.1% Triton X-100) with 100 μg pNPP per reaction at 37 °C for the required time. The reaction was stopped by adding 2 M NaOH, and the absorbance was measured at 405 nm.

For serine/threonine phosphatases, the cells were lysed for 20 min at 4 °C in lysis buffer (15 mM Hepes pH 7.4, 150 mM NaCl, 1 mM EGTA, 0.1 mM $MgCl_2$ and 1% Triton X-100 with 10 $\mu g \cdot mL^{-1}$ each of aprotinin and pepstatin). The assay was carried out using Upstate Ser/Thr phosphatase assay kit according to the instructions provided by manufacturer in the kit protocol.

The individual phosphatases were immunoprecipitated from the respective cytoplasmic fractions by incubating with 1 μg of respective antibody for 2 h at 4 °C, followed by the addition of 40 μL of protein A-Sepharose for another 2 h. The resultant immunoprecipitates were assayed for phosphatase activity using respective assay protocol.

Isolation of RNA and RT-PCR

RNA was isolated from the treated cells (1×10^6) at indicated time points using Trizol reagent according to manufacturer's recommendations. Two microgram of RNA from each group was subjected to reverse transcription using oligo$(dT)_{20}$ and Superscript II Reverse Transcriptase (Invitrogen). The cDNAs were amplified by PCR with appropriate primers. The sequence of primers used for PCR amplification of different genes is given in supplementary Table S1.

ERK kinase assay

For kinase assay, ERK 1/2 was immunoprecipitated from J774.1 cells (1×10^7/time point/treatment). The immunoprecipitates were washed and then incubated in the kinase reaction buffer [20 mM Tris (pH 7.5), 20 mm $MgCl_2$, 2 mM dithiothreitol, 10 μM unlabelled ATP and 10 $\mu Ci \cdot tube^{-1}$ of [^{32}P]-ATP]. The reaction was initiated by addition of 5 $\mu g \cdot tube^{-1}$ of MBP at 30 °C for 10 min or as mentioned. The reaction was terminated by addition of 6× SDS loading buffer followed by boiling for 5 min. The reaction mixtures were subjected to SDS/PAGE. Comparable amounts of ERK1/2 in different groups were ensured by silver staining of the resultant gels. Dried gels were then exposed to X-ray films and amount of [^{32}P]-ATP incorporation in the substrate was ascertained by autoradiography followed by densitometric analysis.

Measurement of reactive oxygen species

Spectrofluorimetry

For spectrofluorimetry, J774A.1 cells (5×10^6 cells in each case) were suspended in 1 mL of serum-free DMEM and labeled with 1 μM of H_2DCFDA for 15 min at 37 °C. Cells were washed twice with medium and re-suspended in 750 μL of medium. The suspension (100 μL) was pipetted into each well of the 96-well plate supplied by the manufacturer. Stimulants were pumped into the wells at the desired time points. The fluorescence was measured by Floustar Optima spectrofluorimeter of BMG laboratories (Offenburg, Germany), using filters that allowed absorption spectrum of 480 nm and emission spectrum of 520 nm.

Flowcytometry

For flowcytometry, the cells (5×10^6 cells in each case) were suspended in 1 mL of medium and labeled with 1 μM of H_2DCFDA for 15 min at 37 °C. Cells were washed twice with medium and resuspended in 1 mL of medium. Treatment was done as applicable and cells were used for FACS analysis at 5- and 10-min time intervals.

Isolation of mouse peritoneal macrophages

Mouse peritoneal macrophages were obtained from resident peritoneal cells of BALB/c mice. The animals were anesthetized and the resident peritoneal cells were harvested, pooled and counted with a hemocytometer. This cell suspension was adjusted to 1×10^6 viable cells per mL in DMEM and incubated for 2 h at 37 °C. The adherent cells were collected and used for further experiments. Experimental procedures requiring animal use were as per the guidelines set out by the Institute for Laboratory Animal Research (Washington DC) [67] and approved by the Institutional Animal Ethics Committee.

Acknowledgements

This work was generously supported by R & D grants to PS from Department of Biotechnology (Government

of India), New Delhi; SKB and NG are recipients of Senior Research Fellowship from Council of Scientific and Industrial Research (CSIR), Government of India. DK and DKS are recipients of the Shyama Prasad Mukherjee (SPM) Fellowship from CSIR, Government of India. The authors have no conflicting financial interests.

References

1 Russell DG (2001) *Mycobacterium tuberculosis*: here today, and here tomorrow. *Nat Rev Mol Cell Biol* **2**, 569–577.
2 Saha B, Das G, Vohra H, Ganguly NK & Mishra GC (1994) Macrophage–T cell interaction in experimental mycobacterial infection. Selective regulation of co-stimulatory molecules on Mycobacterium-infected macrophages and its implication in the suppression of cell-mediated immune response. *Eur J Immunol* **24**, 2618–2624.
3 Hmama Z, Gabathuler R, Jefferies WA, de Jong G & Reiner NE (1998) Attenuation of HLA-DR expression by mononuclear phagocytes infected with *Mycobacterium tuberculosis* is related to intracellular sequestration of immature class II heterodimers. *J Immunol* **161**, 4882–4893.
4 Noss EH, Harding CV & Boom WH (2000) *Mycobacterium tuberculosis* inhibits MHC class II antigen processing in murine bone marrow macrophages. *Cell Immunol* **201**, 63–74.
5 Torres M, Ramachandra L, Rojas RE, Bobadilla K, Thomas J, Canaday DH, Harding CV & Boom WH (2006) Role of phagosomes and major histocompatibility complex class II (MHC-II) compartment in MHC-II antigen processing of *Mycobacterium tuberculosis* in human macrophages. *Infect Immun* **74**, 1621–1630.
6 Sturgill-Koszycki S, Schlesinger PH, Chakraborty P, Haddix PL, Collins HL, Fok AK, Allen RD, Gluck SL, Heuser J & Russell DG (1994) Lack of acidification in Mycobacterium phagosomes produced by exclusion of the vesicular proton-ATPase. *Science* **263**, 678–681.
7 Vergne I, Chua J, Lee HH, Lucas M, Belisle J & Deretic V (2005) Mechanism of phagolysosome biogenesis block by viable *Mycobacterium tuberculosis*. *Proc Natl Acad Sci USA* **102**, 4033–4038.
8 Pieters J (2001) Entry and survival of pathogenic mycobacteria in macrophages. *Microbes Infect* **3**, 249–255.
9 Russell DG (2005) *Mycobacterium tuberculosis*: the Indigestible Microbe. In *Tuberculosis and the Tubercle Bacillus* (Cole ST, Eisenach KD, McMurray DN & Jacobs WR Jr, eds), pp. 427–435. ASM Press, Washington DC.
10 Koul A, Herget T, Klebl B & Ullrich A (2004) Interplay between mycobacteria and host signalling pathways. *Nat Rev Microbiol* **2**, 189–202.
11 Pai RK, Convery M, Hamilton TA, Boom WH & Harding CV (2003) Inhibition of IFN-gamma-induced class II transactivator expression by a 19-kDa lipoprotein from *Mycobacterium tuberculosis*: a potential mechanism for immune evasion. *J Immunol* **171**, 175–184.
12 Knutson KL, Hmama Z, Herrera-Velit P, Rochford R & Reiner NE (1998) Lipoarabinomannan of *Mycobacterium tuberculosis* promotes protein tyrosine dephosphorylation and inhibition of mitogen-activated protein kinase in human mononuclear phagocytes. Role of the Src homology 2 containing tyrosine phosphatase 1. *J Biol Chem* **273**, 645–652.
13 Fratti RA, Chua J, Vergne I & Deretic V (2003) *Mycobacterium tuberculosis* glycosylated phosphatidylinositol causes phagosome maturation arrest. *Proc Natl Acad Sci USA* **100**, 5437–5442.
14 Trajkovic V, Natarajan K & Sharma P (2004) Immunomodulatory action of mycobacterial secretory proteins. *Microbes Infect* **6**, 513–519.
15 Cole ST, Brosch R, Parkhill J, Garnier T, Churcher C, Harris D, Gordon SV, Eiglmeier K, Gas S, Barry CE, *et al.* (1998) Deciphering the biology of *Mycobacterium tuberculosis* from the complete genome sequence. *Nature* **393**, 537–544.
16 Berthet FX, Rasmussen PB, Rosenkrands I, Andersen P & Gicquel B (1998) A *Mycobacterium tuberculosis* operon encoding ESAT-6 and a novel low-molecular-mass culture filtrate protein (CFP-10). *Microbiology* **144**, 3195–3203.
17 Mahairas GG, Sabo PJ, Hickey MJ, Singh DC & Stover CK (1996) Molecular analysis of genetic differences between Mycobacterium bovis BCG and virulent M. bovis. *J Bacteriol* **178**, 1274–1282.
18 Behr MA, Wilson MA, Gill WP, Salamon H, Schoolnik GK, Rane S & Small PM (1999) Comparative genomics of BCG vaccines by whole-genome DNA microarray. *Science* **284**, 1520–1523.
19 Gordon SV, Brosch R, Billault A, Garnier T, Eiglmeier K & Cole ST (1999) Identification of variable regions in the genomes of tubercle bacilli using bacterial artificial chromosome arrays. *Mol Microbiol* **32**, 643–655.
20 Hsu T, Hingley-Wilson SM, Chen B, Chen M, Dai AZ, Morin PM, Marks CB, Padiyar J, Goulding C, Gingery M, *et al.* (2003) The primary mechanism of attenuation of bacillus Calmette–Guerin is a loss of secreted lytic function required for invasion of lung interstitial tissue. *Proc Natl Acad Sci USA* **100**, 12420–12425.
21 Pym AS, Brodin P, Majlessi L, Brosch R, Demangel C, Williams A, Griffiths KE, Marchal G, Leclerc C & Cole ST (2003) Recombinant BCG exporting ESAT-6 confers enhanced protection against tuberculosis. *Nat Med* **9**, 533–539.

22 Stanley SA, Raghavan S, Hwang WW & Cox JS (2003) Acute infection and macrophage subversion by *Mycobacterium tuberculosis* require a specialized secretion system. *Proc Natl Acad Sci USA* **100**, 13001–13006.
23 Guinn KM, Hickey MJ, Mathur SK, Zakel KL, Grotzke JE, Lewinsohn DM, Smith S & Sherman DR (2004) Individual RD1-region genes are required for export of ESAT-6/CFP-10 and for virulence of *Mycobacterium tuberculosis*. *Mol Microbiol* **51**, 359–370.
24 Lewis KN, Liao R, Guinn KM, Hickey MJ, Smith S, Behr MA & Sherman DR (2003) Deletion of RD1 from *Mycobacterium tuberculosis* mimics bacille Calmette–Guerin attenuation. *J Infect Dis* **187**, 117–123.
25 Brodin P, Majlessi L, Brosch R, Smith D, Bancroft G, Clark S, Williams A, Leclerc C & Cole ST (2004) Enhanced protection against tuberculosis by vaccination with recombinant *Mycobacterium microti* vaccine that induces T cell immunity against region of difference 1 antigens. *J Infect Dis* **190**, 115–122.
26 Trajkovic V, Singh G, Singh B, Singh S & Sharma P (2002) Effect of *Mycobacterium tuberculosis*-specific 10-kilodalton antigen on macrophage release of tumor necrosis factor alpha and nitric oxide. *Infect Immun* **70**, 6558–6566.
27 Renshaw PS, Lightbody KL, Veverka V, Muskett FW, Kelly G, Frenkiel TA, Gordon SV, Hewinson RG, Burke B, Norman J, *et al.* (2005) Structure and function of the complex formed by the tuberculosis virulence factors CFP-10 and ESAT-6. *Embo J* **24**, 2491–2498.
28 Zhang Z-Y (1995) Are protein tyrosine phosphatases specific for phosphotyrosine? *J Biol Chem* **270**, 16052–16055.
29 Bannwarth W & Kitas EA (1992) Synthesis of multi-O^4-phospho-L-tyrosine-containing peptides. *Helv Chim Acta* **75**, 707–714.
30 Higashi H, Tsutsumi R, Muto S, Sugiyama T, Azuma T, Asaka M & Hatakeyama M (2002) SHP-2 tyrosine phosphatase as an intracellular target of *Helicobacter pylori* CagA protein. *Science* **295**, 683–686.
31 Singh DK, Kumar D, Siddiqui Z, Basu SK, Kumar V & Rao KV (2005) The strength of receptor signaling is centrally controlled through a cooperative loop between Ca_{2+} and an oxidant signal. *Cell* **121**, 281–293.
32 Xu X & Burke SP (1996) Roles of active site residues and NH_2-terminal domain in the catalysis and substrate binding of human Cdc25. *J Biol Chem* **271**, 5118–5124.
33 Fauman E & Saper M (1996) Structure and function of the protein tyrosine phosphatases. *Trends Biochem Sci* **21**, 413–417.
34 Bretz JR, Mock NM, Charity JC, Zeyad S, Baker CJ & Hutcheson SW (2003) A translocated protein tyrosine phosphatase of *Pseudomonas syringae* pv. *tomato* DC3000 modulates plant defence response to infection. *Mol Microbiol* **49**, 389–400.
35 Babior BM, Kipnes RS & Curnutte JT (1973) Biological defense mechanisms. The production by leukocytes of superoxide, a potential bactericidal agent. *J Clin Invest* **52**, 741–744.
36 Kaul N & Forman HJ (1996) Activation of NF kappa B by the respiratory burst of macrophages. *Free Radic Biol Med* **21**, 401–405.
37 Forman HJ & Torres M (2002) Reactive oxygen species and cell signaling: respiratory burst in macrophage signalling. *Am J Respir Crit Care Med* **166**, S4–S8.
38 Reth M (2002) Hydrogen peroxide as second messenger in lymphocyte activation. *Nat Immunol* **3**, 1129–1134.
39 Finkel T (2003) Oxidant signals and oxidative stress. *Curr Opin Cell Biol* **15**, 247–254.
40 Nathan C (2003) Specificity of a third kind: reactive oxygen and nitrogen intermediates in cell signalling. *J Clin Invest* **111**, 769–778.
41 Singh B, Singh G, Trajkovic V & Sharma P (2003) Intracellular expression of *Mycobacterium tuberculosis*-specific 10-kDa antigen down-regulates macrophage B7.1 expression and nitric oxide release. *Clin Exp Immunol* **134**, 70–77.
42 Ostman A & Bohmer FD (2001) Regulation of receptor tyrosine kinase signaling by protein tyrosine phosphatases. *Trends Cell Biol* **11**, 258–266.
43 Salmeen A & Barford D (2005) Functions and mechanisms of redox regulation of cysteine-based phosphatases. *Antioxid Redox Signal* **7**, 560–577.
44 King MM & Huang CY (1984) The calmodulin-dependent activation and deactivation of the phosphoprotein calcineurin and the effect of nucleotides, pyrophosphate and divalent metal ions. *J Biol Chem* **259**, 8847–8856.
45 Namgaladze D, Hofer HW & Ullrich V (2002) Redox control of calcineurin by targeting binuclear Fe^{2+}–Zn^{2+} center at the enzyme active site. *J Biol Chem* **277**, 5962–5969.
46 Knodler LA, Celli J & Finlay BB (2001) Pathogenic trickery: deception of host cell processes. *Nat Rev Mol Cell Biol* **2**, 578–588.
47 Hornef MW, Wick MJ, Rhen M & Normark S (2002) Bacterial strategies for overcoming host innate and adaptive immune responses. *Nat Immunol* **3**, 1033–1040.
48 Chan ED, Morris KR, Belisle JT, Hill P, Remigio LK, Brennan PJ & Riches DW (2001) Induction of inducible nitric oxide synthase-NO* by lipoarabinomannan of *Mycobacterium tuberculosis* is mediated by MEK1-ERK, MKK7-JNK, and NF-kappaB signaling pathways. *Infect Immun* **69**, 2001–2010.
49 Roach SK & Schorey JS (2002) Differential regulation of the mitogen-activated protein kinases by pathogenic and nonpathogenic mycobacteria. *Infect Immun* **70**, 3040–3052.

50 Brivanlou AH & Darnell JE Jr (2002) Signal transduction and the control of gene expression. *Science* **295**, 813–818.
51 Ehrt S, Schnappinger D, Bekiranov S, Drenkow J, Shi S, Gingeras TR, Gaasterland T, Schoolnik G & Nathan C (2001) Reprogramming of the macrophage transcriptome in response to interferon-gamma and *Mycobacterium tuberculosis*: signaling roles of nitric oxide synthase-2 and phagocyte oxidase. *J Exp Med* **194**, 1123–1140.
52 Ting LM, Kim AC, Cattamanchi A & Ernst JD (1999) *Mycobacterium tuberculosis* inhibits IFN-gamma transcriptional responses without inhibiting activation of STAT1. *J Immunol* **163**, 3898–3906.
53 Zhang SQ, Tsiaras WG, Araki T, Wen G, Minichiello L, Klein R & Neel BG (2002) Receptor-specific regulation of phosphatidylinositol 3′-kinase activation by the protein tyrosine phosphatase Shp2. *Mol Cell Biol* **22**, 4062–4072.
54 Araki T, Nawa H & Neel BG (2003) Tyrosyl phosphorylation of Shp2 is required for normal ERK activation in response to some, but not all, growth factors. *J Biol Chem* **278**, 41677–41684.
55 Kamata T, Yamashita M, Kimura M, Murata K, Inami M, Shimizu C, Sugaya K, Wang CR, Taniguchi M & Nakayama T (2003) src homology 2 domain-containing tyrosine phosphatase SHP-1 controls the development of allergic airway inflammation. *J Clin Invest* **111**, 109–119.
56 Sherman DR, Sabo PJ, Hickey MJ, Arain TM, Mahairas GG, Yuan Y, Barry CE 3rd & Stover CK (1995) Disparate responses to oxidative stress in saprophytic and pathogenic mycobacteria. *Proc Natl Acad Sci USA* **92**, 6625–6629.
57 Manca C, Paul S, Barry CE 3rd, Freedman VH & Kaplan G (1999) Mycobacterium tuberculosis catalase and peroxidase activities and resistance to oxidative killing in human monocytes *in vitro*. *Infect Immun* **67**, 74–79.
58 Zhang Y, Lathigra R, Garbe T, Catty D & Young D (1991) Genetic analysis of superoxide dismutase, the 23 kilodalton antigen of *Mycobacterium tuberculosis*. *Mol Microbiol* **5**, 381–391.
59 Piddington DL, Fang FC, Laessig T, Cooper AM, Orme IM & Buchmeier NA (2001) Cu,Zn superoxide dismutase of *Mycobacterium tuberculosis* contributes to survival in activated macrophages that are generating an oxidative burst. *Infect Immun* **69**, 4980–4987.
60 Renshaw PS, Panagiotidou P, Whelan A, Gordon SV, Hewinson RG, Williamson RA & Carr MD (2002) Conclusive evidence that the major T-cell antigens of the *Mycobacterium tuberculosis* complex ESAT-6 and CFP-10 form a tight, 1: 1 complex and characterization of the structural properties of ESAT-6, CFP-10, and the ESAT-6*CFP-10 complex. Implications for pathogenesis and virulence. *J Biol Chem* **277**, 21598–21603.
61 Gao LY, Guo S, McLaughlin B, Morisaki H, Engel JN & Brown EJ (2004) A mycobacterial virulence gene cluster extending RD1 is required for cytolysis, bacterial spreading and ESAT-6 secretion. *Mol Microbiol* **53**, 1677–1693.
62 Marei A, Ghaemmaghami A, Renshaw P, Wiselka M, Barer M, Carr M & Ziegler-Heitbrock L (2005) Superior T cell activation by ESAT-6 as compared with the ESAT-6-CFP-10 complex. *Int Immunol* **17**, 1439–1446.
63 Okkels LM, Muller EC, Schmid M, Rosenkrands I, Kaufmann SH, Andersen P & Jungblut PR (2004) CFP10 discriminates between nonacetylated and acetylated ESAT-6 of *Mycobacterium tuberculosis* by differential interaction. *Proteomics* **4**, 2954–2960.
64 Gorg A, Obermaier C, Boguth G, Harder A, Scheibe B, Wildgruber R & Weiss W (2000) The current state of two-dimensional electrophoresis with immobilized pH gradients. *Electrophoresis* **21**, 1037–1053.
65 Singh G, Singh B, Trajkovic V & Sharma P (2005) *Mycobacterium tuberculosis* 6-kDa early secreted antigenic target (ESAT-6) protein stimulates activation of J774 macrophages. Immunol Lett **98**, 180–188.
66 Yoshida K & Kufe D (2001) Negative regulation of the SHPTP1 protein tyrosine phosphatase by protein kinase C delta in response to DNA damage. *Mol Pharmacol* **60**, 1431–1438.
67 National Research Council (1996) *Guide for care and use of laboratory animals*. National Academy Press, Washington DC.

Supplementary material

The following supplementary material is available online:

Fig. S1. MTSA-10 induced dephosphorylation is a global phenomenon. The figure shows a diagrammatic illustration of relative change in phosphorylation levels of the individual spots seen in Fig. 1(A). Left end of the line represents the relative phosphorylation level of an individual spot in untreated cells while right end of the line represents the relative phosphorylation level of that spot in MTSA-10-treated cells. An arbitrary scale is used that reflects the relative levels of phosphorylation of each spot. All values represent average of values obtained in three different experiments.

Fig. S2. Effect of MTSA-10 on macrophage ROS generation is a stable phenomenon. (A–F) show the FACS profiles of ROS generation in macrophage as measured by H2DCFDA oxidation in untreated cells (——) and MTSA-10-treated cells (-----). The cells were treated with MTSA-10 for 20 min (A), 40 min (B), 1 h (C), 3 h (D), 6 h (E) and 9 h (F).

Fig. S3. Effect of macrophage ROS generation is MTSA-10 specific. A–D show the FACS profiles of ROS generation as measured by H_2DCFDA oxidation. All treatments were carried out for 10 min. (A) shows ROS FACS profile in untreated J774.1 cells (——), and MTSA-10-treated cells (-----); (B), ROS profiles obtained for untreated cells (——), and ESAT-6 (10 $\mu g \cdot mL^{-1}$)-treated cells (-----); (C), the ROS profiles for untreated cells (solid line), or cells treated simultaneously with MTSA-10 and ESAT-6 (-----), and (D) shows the ROS profiles of untreated cells (——) and MTSA-10–ESAT-6 (1 : 1) complex (10 $\mu g \cdot mL^{-1}$) treated cells (-----). All the figures are representative of three different experiments.

Fig. S4. Regulation of ROS by MTSA-10 is a general phenomenon. The FACS profiles of ROS generation by H_2DCFDA labeled macrophage cells are shown. In (A), FACS profiles of DCFDA labeled untreated RAW 264.7 cells (——) and cells treated with MTSA-10 (-----) are shown. In (B), the profiles of J774.1 cells pretreated with L-*N*-monomethyl arginine (——), and those treated with MTSA-10 (-----) are shown. Data are representative of four experiments.

Fig. S5. MTSA-10 exerts similar effects on primary macrophages. (A–D) show FACS profiles of ROS generation by mouse peritoneal macrophages. All the treatments shown are for 10 min. In (A), profiles for the untreated (——) and MTSA-10 treated (-----) cells are shown; in (B), the ROS profiles for untreated (——) and ESAT-6 (10 $\mu g \cdot mL^{-1}$) treated (-----) cells are shown; in (C), for the untreated (——) and cells treated simultaneously with both MTSA-10 and ESAT-6 (-----) are shown; and in (D), the profile for untreated cells (——) is shown along with that for MTSA-10–ESAT-6 (1 : 1) complex (10 $\mu g \cdot mL^{-1}$)-treated cells. (E) shows the phosphorylation profile of ERK in mouse peritoneal macrophage treated with MTSA-10 for indicated time. The cell lysates representing different treatment times were subjected to western blotting followed by probing with phospho-ERK-specific antibodies. The blots were stripped and reprobed with antibodies against ERK molecule. All the data are representative of three to four different experiments.

Table S1. Nucleotide sequence of the primers used in RT-PCR.

This material is available as part of the online article from http://www.blackwell-synergy.com